

SEMI-ACTIVE MR DAMPERS FOR SEISMIC CONTROL OF STRUCTURES

Jagadish G. Kori¹ and R.S. Jangid²

SUMMARY

Magnetorheological (MR) dampers have been demonstrated to be more effective in reducing the structural response due to earthquakes using only a small amount of external power. The performance of MR damper depends upon type of control law used and the damper force is directly depends on the input command voltage. The purpose of this study is to evaluate the effectiveness of input command voltage on MR damper system against recently proposed control laws under different earthquakes. The magnitude of control force increases with the increase in the input command voltage of MR damper, however for the different damper locations and configurations maximum command voltage to the current driver may not always effective in reducing the structural responses. To investigate the effective performance of the MR dampers, different control algorithms with multiple MR damper locations are considered in this study. A phenomenological model of a shear-mode MR damper, based on a Bouc–Wen element, is employed in the analysis of the controlled building. The control algorithms are tested on a five-story framed building and parametric study on variation in the input command voltage is conducted for different real earthquake ground motions. The numerically evaluated optimum parametric values are considered for the analysis of the different damper locations in the building in order to reduce the displacement, acceleration and the base shear of the building. It is shown numerically that the performance of the MR damper has a great potential in suppressing structural vibrations over a wide range of seismic inputs by selecting appropriate optimum input command voltages.

KEY WORDS

Structural control, semi-active control, MR damper, earthquake, control algorithm

1. INTRODUCTION

Most of the civil engineering structures have very little damping capability; hence extensive damage and even structural failures are common under seismic load. To dissipate energy from earthquakes and reduce vibrations in structures, thereby reducing human and material losses, control devices have been developed and implemented in civil engineering structures. The structural control devices are classified as passive, active and semi-active control (Housner *et al.* 1997), (Datta 2003). One of the more promising among the control devices is the semi-active control device in seismic control of structures known for its simplicity, reliability and small power requirements. Therefore the semi-active control devices have attracted a great deal of attention in recent years. Many of these systems can operate on battery-power alone, proving advantageous during seismic events when the main power source to the structure may fail. Also, because semi-active devices cannot inject energy into the structural system, they do not have the potential to destabilize the system (Spencer and Nagarajaiah 2003). The semi-active control devices are classified as semi-active variable-stiffness systems, semi-active friction control devices, variable orifice dampers and controllable fluid devices.

One of the types of controllable fluid devices is the magnetorheological (MR) damper, which consists of a hydraulic cylinder containing a solution that, in the presence of a magnetic field, can reversibly change from a free-flowing,

linear viscous fluid to a semi-solid state with controllable yield strength. Intensive theoretical and experimental researches have been made on the dynamic behaviour and potential application of MR dampers (Symans and Constantinou 1999). The effective control of structural systems is highly dependent on the control method used for designing the MR damper control law (Dyke and Spencer 1997). The MR dampers can be controlled with low power (e.g., less than 50 W), low voltage (e.g., 12–24 V), current-driven power supply outputting only (e.g., 1–2 A), which could be supplied by batteries and are capable of generating large control forces required for full-scale applications (Dyke *et al.* 1998). The MR dampers are significantly hindered by their inherently hysteretic and highly non-linear dynamics. Hence an appropriate modeling of MR dampers is very important for their application.

Many studies on MR dampers have been conducted analytically as well as experimentally for vibration reduction under wind and earthquakes. Spencer *et al.* (1996), Dyke *et al.* (1996, 1998) and Jansen and Dyke (2000) used MR dampers to reduce the seismic vibrations of model building structures. Yang *et al.* (2002) have developed a large-scale MR damper device that could be applicable to realistic civil and architectural structures. Yoshioka *et al.* (2002), (Faruque Ali and Ramaswamy 2009) incorporated an MR damper with a base isolation system such that the isolation system would be effective under both strong and moderate earthquakes. Yoshida and Dyke (2004) applied semi-active control systems using MR dampers to a non-linear model of a full-scale building to verify its effectiveness in reducing responses when non-linear behaviour is considered. Ohtori *et al.* (2004) used a model of a full-scale 20-story building model developed for

¹ Principal Saraswati College of Engineering, Kharghar, Navi-Mumbai-410210 (India)

² Professor Department of Civil Engineering, Indian Institute of Technology Bombay, Powai, Mumbai – 400 076 (India) (e-mail: rsjangid@civil.iitb.ac.in)

the benchmark control problem for seismically excited non-linear buildings. Yoshida and Dyke (2005) investigated the placement scheme of MR dampers based on genetic algorithms (GA). Soneji and Jangid (2006) studied the effectiveness of semi-active MR dampers in reducing the seismic response of cable-stayed bridges.

Several models have been proposed to describe the behaviour of the MR damper. These include the phenomenological model based on a Bouc–Wen hysteresis model proposed by Spencer *et al.* (1997), neural network model developed by Chang and Roschke (1998), viscoelastic–plastic model (Wereley *et al.*, 1998), fuzzy model (Schurter and Roschke, 2000), (Huang *et al.*, 2009), polynomial model (Choi *et al.*, 2001). Among these MR models, the phenomenological model can accurately describe the behaviour of the MR dampers. Neural network and fuzzy models can be used for the MR dampers, but the selection of network structure and training data are essential in order to obtain accurate results. In the viscoelastic–plastic model the inverse dynamics of the MR dampers are often difficult to obtain due to their nonlinear characteristics. The limitation of polynomial models is that it cannot characterize the MR behaviour favorably at the relatively low velocity region.

In this paper, the model consisting of a Bouc–Wen element in parallel with a viscous damper predicts the behaviour of a shear-mode MR damper proposed by (Yoshida and Dyke, 2004) is used. The device consists of two steel parallel plates. The magnetic field produced in the device is generated by an electromagnet consisting of a coil at one end of the device. Forces are generated when the moving plate, coated with thin foam saturated with MR fluid, slides between the two parallel plates. The damper force increases with increasing magnetic field and is dependent on the command voltage. The maximum command voltage is fixed with respect to the saturation of magnetic field in the MR fluid damper. The force generated by the MR fluid damper cannot be commanded directly; only the command voltage applied to the current driver of the MR fluid damper can be directly controlled. The response of the MR damper is dependent on the local motion of the structure and also on the maximum input command voltage to the current driver. Hence it is important to know the optimum input command voltage, so that resulting MR damper force in a structural system causes a reduction in the structural responses. The optimum command voltage can be any value between 0 and V_{\max} . So far, the effect of command voltage on the MR damper and the evaluation of optimal value based on the different configuration of damper locations under different earthquake loadings have not been investigated. The aim of this paper is to compare some of the MR damper control algorithms by conducting a critical parametric study in the vibration control of structures. Here the influence of variation in command voltage of the MR damper for the seismic response of a structure is considered for different earthquake ground motions. The primary objectives of this study can be summarized as: (i) to investigate the effect of command voltage in a semi-active MR damper, which is critical in determining the effectiveness to structural vibration control, (ii) to identify the optimal value of command voltage for the best possible structural control configurations with different damper deployments, (iii) to evaluate analytically the dynamics of semi-active MR dampers for various semi-active control algorithms, that can provide better performance with the change in input command voltage and (iv) to suggest effective guidelines for the use of semi-active MR dampers in vibration control of structures based on the parametric study.

2. MODEL OF MAGNETORHEOLOGICAL DAMPER

The MR dampers show dynamically non-linear force-velocity behaviour, hence a more accurate dynamic model of MR dampers is necessary. Also modeling of the control devices is

essential for the adequate prediction of the behaviour of the controlled system. The Bouc–Wen model proposed by Wen (1976) that is numerically tractable and has been used extensively for modeling the hysteretic system and has been considered for describing the behaviour of the MR damper. The Bouc–Wen model is extremely versatile and can exhibit a wide variety of hysteretic behaviour. A schematic of the shear-mode MR damper model is shown in Figure 1(a).

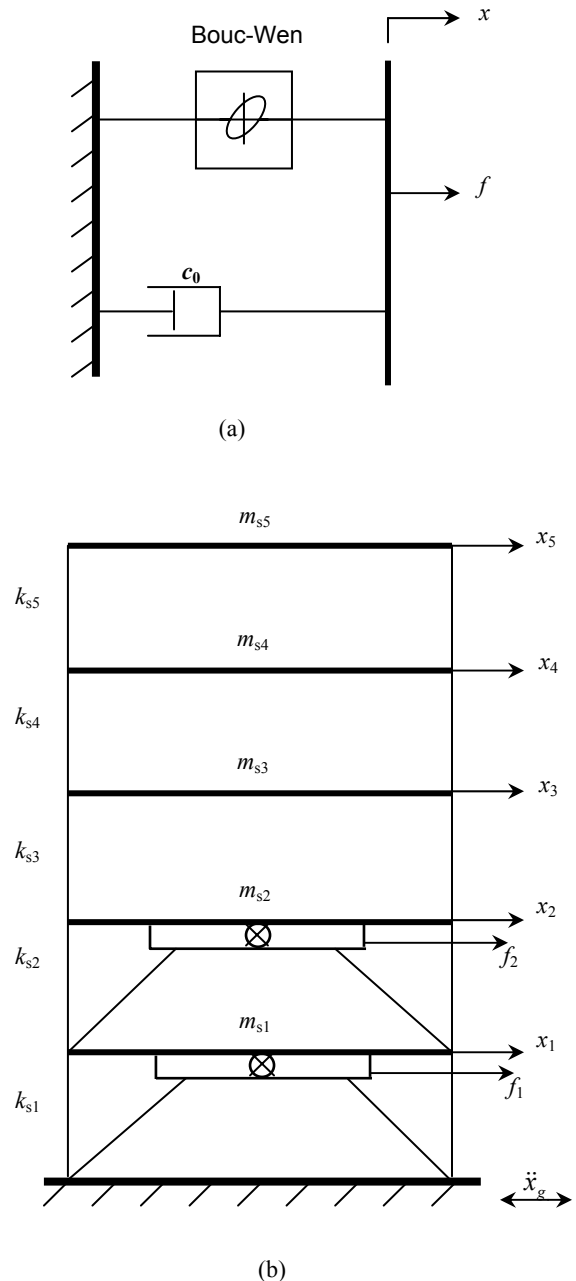


Figure 1. Model of shear-mode MR damper and five-story building with MR dampers.

The model consisting of a Bouc–Wen element in parallel with a viscous damper predicts the behaviour of a shear-mode MR damper. The expression governing the force predicted by this model is as follows

$$f = c_0 \dot{x} + \alpha z \quad (1)$$

$$\dot{z} = -\gamma |\dot{x}| |z|^{n-1} - \beta \dot{x} |z|^n + A \dot{x} \quad (2)$$

where z is an evolutionary variable that accounts for the history dependence of the response and x is the damper displacement. The parameters c_0 , α , β , γ , n and A are called the shape or characteristic parameters of the model. The model parameters α and c_0 depend on the voltage to the current driver as follows

$$\alpha = \alpha_a + \alpha_b u, \quad c_0 = c_{0a} + c_{0b} u \quad (3)$$

while the filtered voltage u is determined by the applied voltage v as follows

$$\dot{u} = -\eta(u - v) \quad (4)$$

where η is a constant. Equation 4 is necessary to model the dynamics involved in reaching rheological equilibrium and in driving the electromagnet in the MR damper.

3. GOVERNING EQUATIONS OF MOTION

Consider a multi-story building equipped with semi-active MR dampers as shown in Figure 1(b). The notations m_i , k_i and x_i in Figure 1(b) represent the mass, stiffness and displacement relative-to-the-ground of the i -th floor. Assuming that the forces provided by the MR damper are adequate to keep the response of the primary structure from exiting the linear region, and then the equations of motion can be written as

$$\mathbf{M}_s \ddot{\mathbf{x}} + \mathbf{C}_s \dot{\mathbf{x}} + \mathbf{K}_s \mathbf{x} = \mathbf{\Lambda} \mathbf{f} - \mathbf{M}_s \mathbf{\Gamma} \ddot{\mathbf{x}}_g \quad (5)$$

where \mathbf{M}_s is the mass matrix, \mathbf{C}_s is the damping matrix, \mathbf{K}_s is the stiffness matrix, \mathbf{x} is the vector of floor displacements, $\dot{\mathbf{x}}$ and $\ddot{\mathbf{x}}$ are floor velocity and acceleration vectors, respectively, $\mathbf{\Lambda}$ is a matrix of zeros and ones, where one will indicate where the MR damper force is being applied, $\mathbf{f} = [f_1, f_2, \dots, f_n]^T$ is the vector of control force produced by the dampers, $\mathbf{\Gamma}$ is a vector of ones and $\ddot{\mathbf{x}}_g$ is the acceleration due to an earthquake. For the uncontrolled case, the force \mathbf{f} produced by the MR damper is zero. Using the state-space representation Equation 5 takes the following form

$$\dot{\mathbf{z}}_y = \mathbf{A} \mathbf{z}_y + \mathbf{B} \mathbf{f} + \mathbf{E} \ddot{\mathbf{x}}_g \quad (6)$$

$$\mathbf{y} = \mathbf{C} \mathbf{z}_y + \mathbf{D} \mathbf{f} + \mathbf{v} \quad (7)$$

where $\mathbf{z}_y = [\mathbf{x} \ \dot{\mathbf{x}}]^T$ is the state vector, $\mathbf{y} = [\ddot{\mathbf{x}} \ \mathbf{x}]^T$ is the vector of measured outputs, and \mathbf{v} is the measurement noise vector. The system matrices are defined as follows

$$\mathbf{A} = \begin{bmatrix} \mathbf{0} & \mathbf{I} \\ -\mathbf{M}_s^{-1} \mathbf{K}_s & -\mathbf{M}_s^{-1} \mathbf{C}_s \end{bmatrix}, \quad \mathbf{B} = \begin{bmatrix} \mathbf{0} \\ \mathbf{M}_s^{-1} \mathbf{\Lambda} \end{bmatrix}, \quad \mathbf{E} = -\begin{bmatrix} \mathbf{0} \\ \mathbf{\Gamma} \end{bmatrix} \quad (8)$$

$$\mathbf{C} = \begin{bmatrix} -\mathbf{M}_s^{-1} \mathbf{K}_s & -\mathbf{M}_s^{-1} \mathbf{C}_s \\ \mathbf{I} & \mathbf{0} \end{bmatrix},$$

$$\mathbf{D} = \begin{bmatrix} -\mathbf{M}_s^{-1} \mathbf{\Lambda} \\ \mathbf{0} \end{bmatrix} \quad (9)$$

4. SEMI-ACTIVE CONTROL ALGORITHM

Semi-active control systems are typically highly non-linear. One of the main challenges in semi-active control is the development of an appropriate control algorithm that can take advantage of the features of the control device to produce an effective control system. To evaluate the performance of semi-active control algorithms, here three versatile and effective control algorithms are selected in the current study. These three control algorithms; the bang-bang controller, the Lyapunov controller and Clipped-Optimal controller are described in this section.

Bang-bang control algorithm

In this approach, requires measurements of the floor velocities and applied forces. The control strategy based on Lyapunov function to represent the total vibratory energy in the structure and this control algorithm determines the current sent to the i^{th} MR damper as follows

$$v_i = V_{\max} H(-(\dot{\mathbf{x}} + \mathbf{\Gamma} \dot{\mathbf{x}}_g)^T \mathbf{\Lambda}_i f_i) \quad (10)$$

where $H(\cdot)$ is the Heaviside step function. Here $\mathbf{\Lambda}_i$ is the i^{th} column of the $\mathbf{\Lambda}$ matrix.

Lyapunov stability theory control algorithm

This approach requires the use of a Lyapunov function; even though numbers of Lyapunov functions are available, but here Lyapunov's direct approach is used, in which a positive definite matrix \mathbf{P} is found with selected positive semi-definite matrix \mathbf{Q}_p by using the following Lyapunov equation.

$$\mathbf{A}^T \mathbf{P} + \mathbf{P} \mathbf{A} = -\mathbf{Q}_p \quad (11)$$

The control law determines the current sent to i^{th} MR damper is as follows

$$v_i = V_{\max} H((-z_y)^T \mathbf{P} \mathbf{B}_i f_i) \quad (12)$$

Clipped-optimal control algorithm

The clipped-optimal control strategy is based on acceleration feedback for controlling the MR dampers. In this approach a linear optimal controller, $\mathbf{K}_c(s)$ is designed that calculates the vector of desired control forces, $\mathbf{f}_c = [f_{c1}, f_{c2}, \dots, f_{cn}]^T$ based on the measured structural response vector, \mathbf{y} and the measured control force vector, \mathbf{f} applied to the structure as follows

$$\mathbf{f}_c = L^{-1} \left\{ -\mathbf{K}_c(s) L \begin{Bmatrix} \mathbf{y} \\ \mathbf{f} \end{Bmatrix} \right\} \quad (13)$$

where $L\{\cdot\}$ is the Laplace transform. The optimal controller $\mathbf{K}_c(s)$ is obtained from H_2/LQG method. The command signal v for i^{th} MR damper is selected according to the following control law

$$v_i = V_{\max} H(\{f_{C_i} - f_i\} f_i) \quad (14)$$

In this application, the measurements typically available for control force determination include the acceleration of selected points on the structure, the displacement of the MR dampers and the measurement of the control forces provided by the MR dampers. In general, the control algorithms for the dampers may require that the dampers perform work on the structure such that the energy within the structural system is increased. In developing the control laws, the command voltage is restricted to the range $V \in [0, V_{\max}]$, and for a fixed set of states, the magnitude of the applied force, f increases when V increases, and decreases when V decreases.

5. NUMERICAL STUDY

To evaluate the performance of MR damper under variation of the command voltage a numerical example is considered. The properties of a five-story building are as follows: (i) the mass of each floor is identical $m_i = 98300$ kg for $i = 1, 2, \dots, 5$; (ii) The stiffness k_i ($i = 1, 2, \dots, 5$) of five story units are 6.84×10^8 , 6.84×10^8 , 6.84×10^8 , 6.84×10^8 , 5.16×10^8 kN/m respectively, and (iii) Damping ratio for each mode of 5%. The seismic response of the structure is studied for four different strong earthquake ground motions: (i) El Centro SE (1940, PGA= 0.348g); (ii) Kobe NE (1995, PGA= 0.834g); (iii) Loma Prieta NE (1989, PGA= 0.57g); and (iv) Northridge NE (1994, PGA= 0.843g).

The damper parameters are as follows, $C_{0a} = 4.40$ N-sec/cm,

$C_{0b} = 44.00$ N-sec/cm/V, $\alpha_a = 1.0872e5$ N/cm, $\alpha_b = 4.9616e5$ N/cm/V, $\gamma = 3$ cm⁻¹, $\beta = 3$ cm⁻¹, $A = 1.2$, $n = 1$, $\eta = 50$ sec⁻¹. The damper parameters used in this study are from Yoshida and Dyke (2004), the maximum MR device capacity of 1,000 kN with maximum command voltage of 10V. To investigate the effect of variation in command voltage in the range 0 to 10 V, a parametric study is performed using the different control algorithms. The effects of parametrical studies are evaluated by comparing dynamic time-history analysis results.

The several possible structural control configurations with different damper deployments are considered for evaluation of the optimum command voltage parameter. Here the placing sequence adopted is one semi-active MR damper between the ground and the first floor and gradually increasing the dampers to all the floors of five-story structures. The various results of voltages are plotted with peak displacement, absolute acceleration, base shear and peak control forces against variation of voltage in the range of 0 to 10V as shown in Figures 2 to 10 under different earthquake ground motions using three different control algorithms.

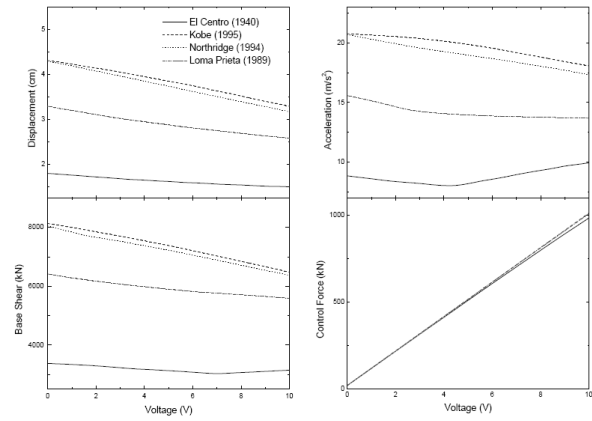


Figure 2. Effect of voltage on peak displacement, acceleration, base shear and control force when MR damper placed at first floor of five-story building subjected to different ground motions for Bang-Bang control algorithm.

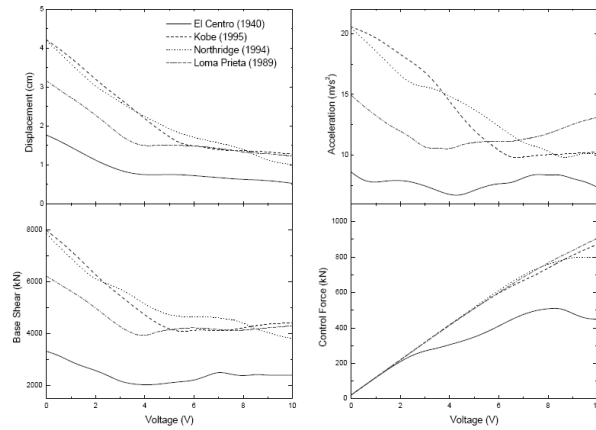


Figure 3. Effect of voltage on peak displacement, acceleration, base shear and control force when MR damper placed at bottom three floors of five-story building subjected to different ground motions for Bang-Bang control algorithm.

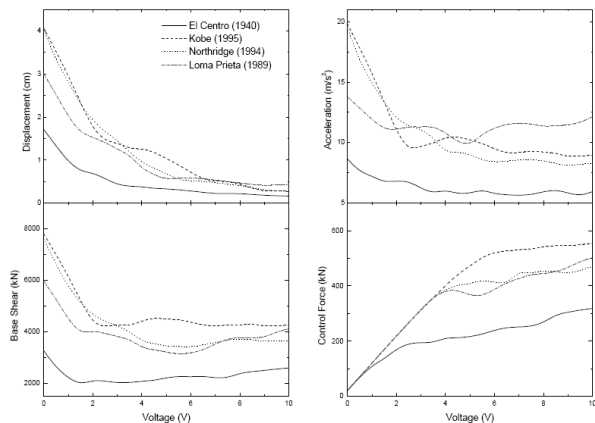


Figure 4. Effect of voltage on peak displacement, acceleration, base shear and control force when MR damper placed at all the floors of five-story building subjected to different ground motions for Bang-Bang control algorithm.

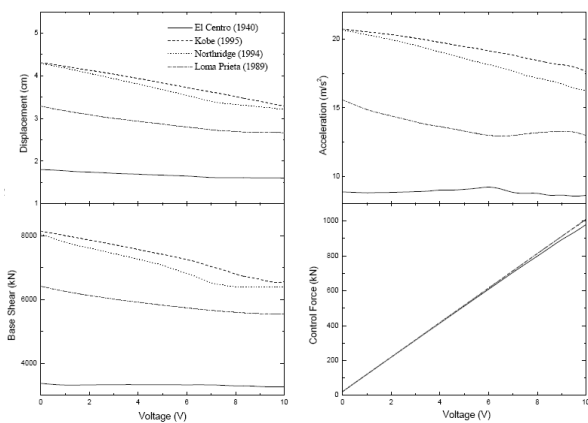


Figure 5. Effect of voltage on peak displacement, acceleration, base shear and control force when MR damper placed at first floor of five-story building subjected to different ground motions for Lyapunov control algorithm.

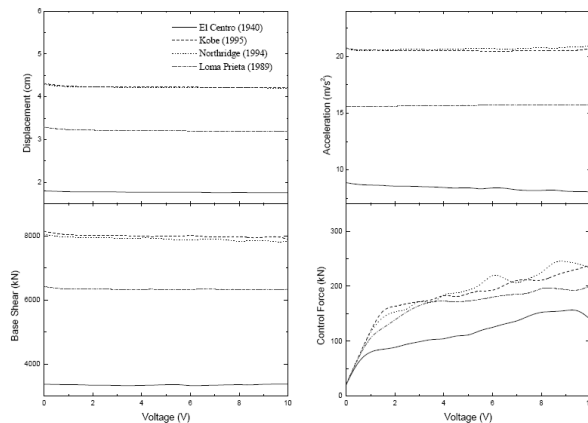


Figure 8. Effect of voltage on peak displacement, acceleration, base shear and control force when MR damper placed at first floor of five-story building subjected to different ground motions for Clipped-optimal control algorithm.

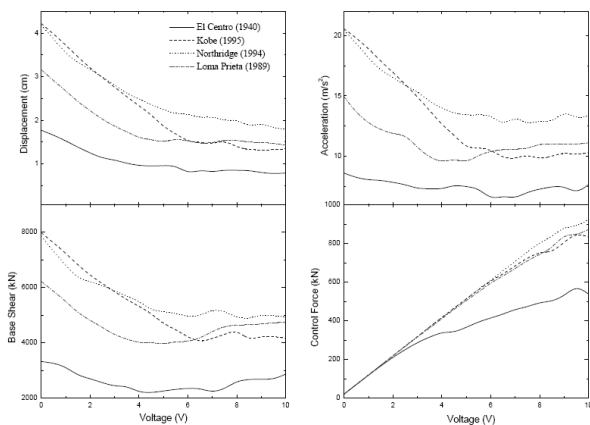


Figure 6. Effect of voltage on peak displacement, acceleration, base shear and control force when MR damper placed at bottom three floors of five-story building subjected to different ground motions for Lyapunov control algorithm.

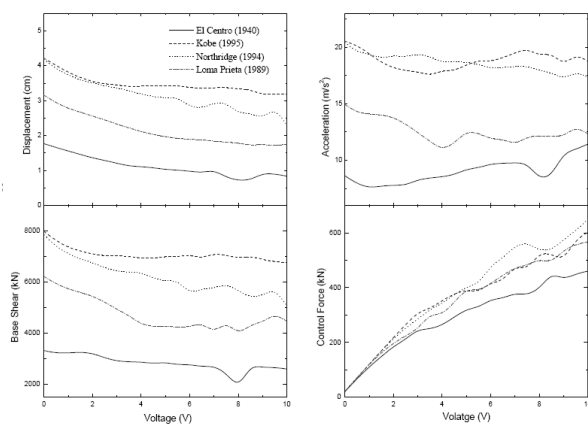


Figure 9. Effect of voltage on peak displacement, acceleration, base shear and control force when MR damper placed at bottom three floors of five-story building subjected to different ground motions for Clipped-optimal control algorithm.

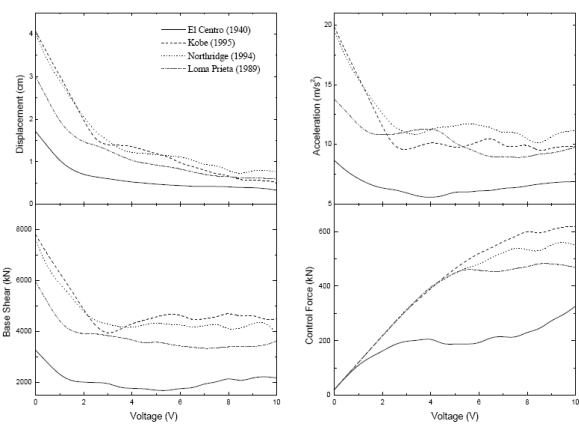


Figure 7. Effect of voltage on peak displacement, acceleration, base shear and control force when MR damper placed at all the floors of five-story building subjected to different ground motions for Lyapunov control algorithm.

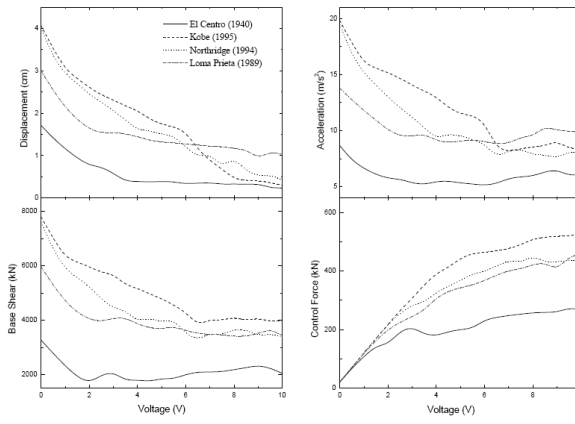


Figure 10. Effect of voltage on peak displacement, acceleration, base shear and control force when MR damper placed at all the floors of five-story building subjected to different ground motions for Clipped-optimal control algorithm.

Table 1. Comparison of 5-story peak structural responses of MR dampers using Bang-bang control algorithm under different ground motions.

Control Type	Damper Placed at	Voltage Input (V_{max})	Displacement (cm)			Acceleration (m/s^2)				
			Imperial Valley	Kobe	Loma Prieta	Northridge	Imperial Valley	Kobe	Loma Prieta	Northridge
Uncontrolled	-	-	1.81	4.33	3.33	4.32	8.97	15.71	20.70	20.70
Passive-OFF	1F	-	1.80	4.31	3.29	4.29	8.88	14.69	20.68	20.68
	1,2F	-	1.78	4.27	3.23	4.25	8.71	15.35	20.64	20.64
	1,2,3F	-	1.76	4.21	3.16	4.19	8.62	14.92	20.44	20.44
	1,2,3,4F	-	1.74	4.15	3.08	4.11	8.63	14.41	20.05	20.05
	1, 2,3,4,5F	-	1.70	4.07	3.00	4.01	8.65	13.77	19.49	19.49
Passive-ON	1F	10V	1.69	4.02	3.02	3.83	8.36	14.21	19.31	19.31
	1,2F	10V	1.13	2.76	2.01	2.87	8.13	12.86	15.95	15.95
	1,2,3F	10V	0.87	1.83	1.83	2.08	7.51	11.01	13.92	13.92
	1,2,3,4F	10V	0.62	1.43	1.34	1.21	6.89	11.96	10.62	10.62
	1, 2,3,4,5F	10V	0.47	1.08	0.61	0.92	6.18	10.25	9.13	9.13
Semi-active	1F	4V	1.64 (8.88)	3.95 (8.35)	2.94 (10.64)	3.84 (10.49)	8.31 (6.41)	14.06 (4.28)	19.26 (6.82)	19.26 (6.82)
	1,2F	6V	1.08 (39.12)	2.62 (38.64)	1.76 (45.51)	2.67 (37.17)	8.06 (7.46)	12.20 (20.52)	15.38 (25.48)	15.38 (25.48)
	1,2,3F	5V	0.76 (56.81)	1.72 (59.14)	1.51 (52.21)	1.92 (54.15)	7.12 (17.41)	11.05 (25.94)	13.75 (32.73)	13.75 (32.73)
	1,2,3,4F	5V	0.43 (75.28)	1.32 (68.43)	1.25 (59.41)	1.10 (73.23)	6.81 (21.08)	11.42 (20.74)	9.45 (52.87)	9.45 (52.87)
	1, 2,3,4,5F	5V	0.33 (80.58)	1.03 (74.69)	0.55 (81.67)	0.68 (83.04)	5.80 (32.96)	9.78 (28.97)	9.04 (53.61)	9.04 (53.61)

Numbers in parentheses denotes the % reduction in responses with the Passive-OFF control system

Table 2. Comparison of 5-story peak structural responses of MR dampers using Lyapunov control algorithm under different ground motions.

Control Type	Damper Placed at	Voltage Input (V_{max})	Displacement (cm)			Acceleration (m/s^2)				
			Imperial Valley	Kobe	Loma Prieta	Northridge	Imperial Valley	Kobe	Loma Prieta	Northridge
Uncontrolled	-	-	1.81	4.33	3.33	4.32	8.97	15.71	20.70	20.70
	1F	-	1.80	4.31	3.29	4.29	8.88	14.69	20.68	20.68
Passive-OFF	1,2F	-	1.78	4.27	3.23	4.25	8.71	15.35	20.64	20.64
	1,2,3F	-	1.76	4.21	3.16	4.19	8.62	14.92	20.44	20.44
	1,2,3,4F	-	1.74	4.15	3.08	4.11	8.63	14.41	20.05	20.05
	1, 2,3,4,5F	-	1.70	4.07	3.00	4.01	8.65	13.77	19.49	19.49
	1F	10V	1.66	3.81	2.91	3.61	8.83	13.51	17.95	17.95
Passive-ON	1,2F	10V	1.38	2.82	2.16	2.92	7.91	11.03	15.21	15.21
	1,2,3F	10V	0.83	1.79	1.62	2.26	6.68	10.79	13.78	13.78
	1,2,3,4F	10V	0.77	1.68	1.53	1.79	6.53	11.21	11.92	11.92
	1, 2,3,4,5F	10V	0.61	1.23	1.03	1.23	6.19	10.14	11.21	11.21
	1F	7V	1.61 (10.55)	3.62 (16.01)	2.73 (17.02)	3.40 (20.74)	8.78 (1.12)	12.95 (11.84)	17.72 (14.31)	17.72 (14.31)
Semi-active	1,2F	6V	1.23 (30.89)	2.61 (38.87)	2.01 (37.77)	2.84 (33.17)	7.84 (9.98)	10.98 (28.40)	15.16 (26.55)	15.16 (26.55)
	1,2,3F	6V	0.78 (55.69)	1.51 (64.13)	1.53 (50.32)	2.15 (48.68)	6.45 (25.17)	10.43 (30.09)	13.44 (34.24)	13.44 (34.24)
	1,2,3,4F	5V	0.69 (60.34)	1.49 (64.09)	1.44 (53.24)	1.75 (57.42)	6.46 (25.14)	11.10 (22.97)	11.24 (43.94)	11.24 (43.94)
	1, 2,3,4,5F	5V	0.47 (72.35)	1.19 (70.76)	0.92 (69.33)	1.16 (71.07)	6.06 (29.94)	10.03 (27.16)	10.15 (49.92)	10.15 (49.92)
	1F	5V	0.47 (72.35)	1.19 (70.76)	0.92 (69.33)	1.16 (71.07)	6.06 (29.94)	10.03 (27.16)	10.15 (49.92)	10.15 (49.92)

Numbers in parentheses denotes the % reduction in responses with the Passive-OFF control system

Table 3. Comparison of 5-story peak structural responses of MR dampers using clipped-optimal control algorithm under different ground motions.

Control Type	Damper Placed at	Voltage Input (V_{max})	Displacement (cm)				Acceleration (m/s^2)			
			Imperial Valley	Kobe	Loma Prieta	Northridge	Imperial Valley	Kobe	Loma Prieta	Northridge
Uncontrolled	-	-	1.81	4.33	3.33	4.32	8.97	15.71	20.70	20.70
	1F	-	1.80	4.31	3.29	4.29	8.88	14.69	20.68	20.68
Passive-OFF	1,2F	-	1.78	4.27	3.23	4.25	8.71	15.35	20.64	20.64
	1,2,3F	-	1.76	4.21	3.16	4.19	8.62	14.92	20.44	20.44
	1,2,3,4F	-	1.74	4.15	3.08	4.11	8.63	14.41	20.05	20.05
	1, 2,3,4,5F	-	1.70	4.07	3.00	4.01	8.65	13.77	19.49	19.49
	1F	10V	1.75	4.27	3.14	4.23	8.69	14.51	20.47	20.47
Passive-ON	1,2F	10V	1.59	4.02	2.91	3.81	8.18	14.58	20.13	20.13
	1,2,3F	10V	1.22	3.68	2.39	3.27	7.86	11.22	19.15	19.15
	1,2,3,4F	10V	0.93	2.94	1.68	2.67	6.94	9.38	15.57	15.57
	1, 2,3,4,5F	10V	0.61	1.73	1.34	1.36	5.26	9.11	9.12	9.12
	1F	2V	1.77	4.23	3.22	4.22	8.54	14.43	20.42	20.42
Semi-active	1,2F	5V	(1.66)	(1.85)	(5.16)	(1.63)	(3.82)	(1.76)	(1.25)	(1.25)
	1,2,3F	4V	1.50	3.65	2.68	3.56	8.06	14.34	20.04	20.04
	1,2,3,4F	4V	(15.73)	(14.52)	(17.02)	(16.23)	(7.46)	(6.57)	(2.90)	(2.90)
	1, 2,3,4,5F	6V	1.11	3.42	2.12	3.19	7.78	10.91	18.63	18.63
	1,2,3,4F	4V	(36.93)	(18.76)	(32.91)	(31.34)	(9.74)	(26.87)	(8.85)	(8.85)
1, 2,3,4,5F	4V	0.73	2.80	1.59	2.44	6.89	9.31	15.15	15.15	15.15
	4V	(58.04)	(32.53)	(48.37)	(40.63)	(20.16)	(35.39)	(24.43)	(24.43)	(24.43)
1, 2,3,4,5F	6V	0.33	1.58	1.27	1.20	5.11	9.02	11.84	11.84	
			(65.88)	(61.67)	(57.67)	(70.05)	(40.97)	(48.83)	(39.25)	(39.25)

Numbers in parentheses denotes the % reduction in responses with the Passive-OFF control system

It is observed from the Figures 2 to 10 that, the command voltage plays an important role in the response of the building and also it varies with different configurations of damper placements. From Figure 2, an optimum value of the command voltage can be found as 4V when the damper is placed at first floor of a five-story building, for the all the responses under the different earthquake ground motions.

Similarly, from Figures 3 to 10, the optimum parameter of voltage can be observed for the Bang-bang, Lyapunov and Clipped-optimal when the dampers are placed at bottom floor to all the floors of a five-story building. Tables 1 to 3 show the peak response quantities for the identified optimum input command voltages to MR dampers under the four real earthquakes ground motions. The overall results indicate that the MR dampers with Bang-Bang, Lyapunov and Clipped-Optimal theory control algorithms under different ground motions achieve a reasonable level of performance as compared to passive ON and OFF devices. The results from Table 1 for the Bang-bang control algorithm with identified optimum command voltage under different ground motions shows maximum story displacement reductions ranging from 74 to 83%, while the maximum story absolute acceleration reductions ranged from 28 to 53%. Similarly, the results from Table 2 for the Lyapunov control algorithm with identified optimum command voltage under different ground motions shows maximum story displacement reductions ranging from 69 to 72%, while maximum absolute acceleration reductions ranged from 27 to 51%. And the results from Table 3 for the Clipped-optimal control algorithm with identified optimum command voltage parameter under different ground motions shows the maximum story displacement reductions ranging from 57 to 70%, while the maximum story absolute acceleration reductions ranged from 34 to 48%. Thus for given configuration, it is also important to note that increasing the number of semi-active dampers from the economic point of view is not desirable. Hence, by comparing results from the Tables 1 to 3, with the minimum number of three MR dampers is more effective to control the structural responses in a five-story building.

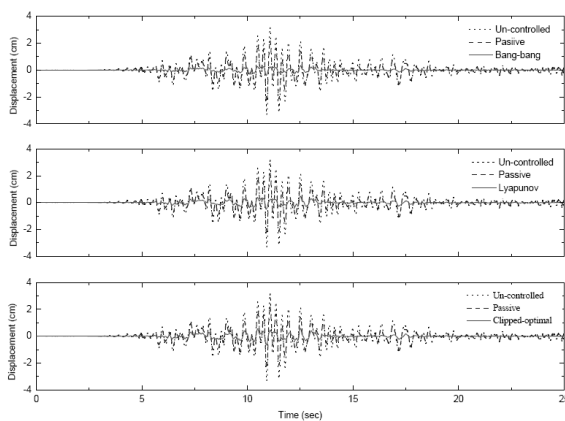


Figure 11. Time-variation of top floor displacement of Un-controlled, Passive and Semi-active MR damper control systems under El Centro (1940) ground motion.

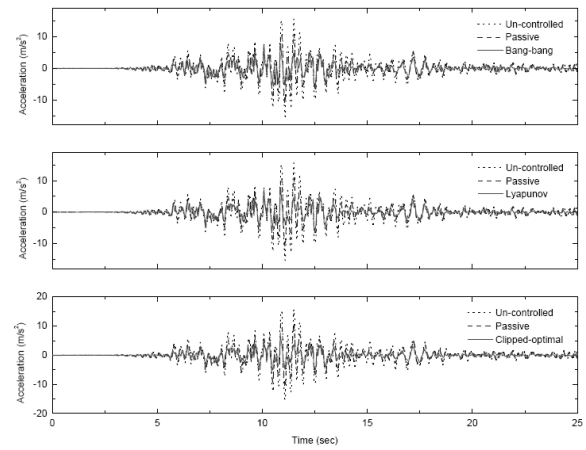


Figure 12. Time-variation of top floor acceleration of Un-controlled, Passive and Semi-active MR damper control systems under El Centro (1940) ground motion.

Figures 11 and 12 compare the time variation of the top story displacements, and the absolute top story acceleration for the uncontrolled building and the building with all the floors with passive dampers/ semi-active dampers under the El Centro (1940) real ground motions. From Figures 11 and 12 it can be seen that the semi-active MR dampers for all control systems are the most effective in reducing the displacement and the acceleration compared to the passive dampers.

6. CONCLUSIONS

For buildings subjected to different types of real earthquakes, the effectiveness and performance of various control algorithms for semi-active MR dampers have been investigated and presented. The parametric study is conducted on a five-story building to observe the influence of variation of the input command voltage in the range 0 to 10V with different configurations of the MR damper deployment positions in buildings, with and without control devices. Comparative performance of different MR control algorithms with the optimum input command voltage parameter is determined under real earthquake ground motions. All control algorithms with using an optimum input command voltage parameter demonstrated its effectiveness in reducing the structural response. From the numerical investigation of the building with MR dampers used as a protective controlling system, the following conclusions may be drawn:

- 1) It is shown from the numerical study that the semi-active MR dampers are quite effective in reducing both the peak displacement and the peak acceleration under different types of real earthquake ground motions.
- 2) From the parametric study, the peak displacements and structural accelerations are reduced with an increase in the input command voltage of the MR dampers. However there exists an optimum value of the voltage input depending upon the damper locations.
- 3) The control algorithms considered for the MR damper, namely, the Bang-bang, the Lyapunov, and the Clipped-optimal imparts reduction in response for the structures. But comparatively the Bang-bang control algorithm performed better for the optimum input command voltage.
- 4) The results show that the building with multiple MR dampers with optimum commanding voltage shows improved seismic response when compared with the passive-ON dampers.

- 5) The scope of this parametric study is to provide information on the efficiency of various MR control algorithm mechanisms with the optimum value of input command voltage so as to suppress the earthquake response.

REFERENCES

1. Bhardwaj, M.K. and Datta, T.K. (2006). "Semi active fuzzy control of the seismic response of building frames", *Journal of Structural Engineering*, **132**(5), 791-799.
2. Chang, C.C. and Roschke, P. (1998). "Neural network modeling of a magnetorheological damper." *Journal of Intelligent Material Systems and Structures*, **9** (9), 755–764.
3. Choi, S.B., Lee, S.K. and Park, Y.P. (2001). "A hysteresis model for the field-dependent damping force of a magnetorheological damper." *Journal of Sound and Vibration*, **245** (2), 375–383.
4. Datta, T.K. (2003). "A state-of-the-art review on active control of structures", *ASET Journal of Earthquake Technology*, **40**(1), 1-17.
5. Dyke, S. J., Spencer, B.F., Jr., Sain, M.K. and Carlson, J.D. (1996). "Modeling and control of magnetorheological dampers for seismic response." *Smart Materials and Structures*, **5**, 565–575.
6. Dyke, S.J. and Spencer, B.F. Jr., (1997). "A Comparison of Semi-Active Control Strategies for the MR Damper." *Proceeding of the IASTED Intl. Conf. on Intelligent Info. Systems*, Bahamas, 580–584.
7. Dyke, S.J., Spencer, B.F., Jr., Sain, M.K. and Carlson, J. D. (1998). "An experimental study of MR dampers for seismic protection." *Smart Materials and Structures*, **7**(5), 693–703.
8. Faruque Ali, S.K. and Ramaswamy, Ananth. (2009). "Hybrid structural control using magnetorheological dampers for base isolated structures", *Smart Materials and Structures*, **18**(5), 5011-16.
9. Housner, G.W., Bergman, L.A., Caughey, T.K., Chassiakos, A.G., Claus, R.O., Masri, R.E., Skelton, S. F., Soong, T.T., Spencer, B.F., Yao, J.T.P. (1997). "Structural control: past, present, and future." *Journal of Engineering Mechanics*, ASCE, **123**, 897–971.
10. Huang, Z.S., Wu, C. and Hsu, D.S. (2009). "Semi-active fuzzy control of MR damper on structures by genetic algorithm", *Journal of Mechanics*, **25**(1), N1-N6.
11. Jansen, L.M. and Dyke, S.J. (2000). "Semi-active control strategies for MR dampers: Comparative study." *Journal of Engineering Mechanics*, ASCE, **126**(8), 795–803.
12. Ohtori, Y., Christenson, R.E., Spencer, B.F., Jr., and Dyke, S.J. (2004). "Benchmark control problems for seismically excited nonlinear buildings." *Journal of Engineering Mechanics*, ASCE, **130**(4), 366–385.
13. Schurter, K.C., and Roschke, P.N. (2000). "Fuzzy modeling of a magnetorheological damper using ANFIS." *Proceedings of the IEEE International Conference on Fuzzy Systems*, 122–127.
14. Soneji, B.B., and Jangid, R.S. (2006). "Seismic control of cable-stayed bridge using semi-active hybrid system." *Bridge Structures*, **2**(1), 45–60.
15. Spencer, Jr., B.F., Dyke, S.J., and Sain, M.K. (1996). "Magnetorheological dampers: a new approach to seismic protection of structures." *Proc. Conf. on Decision and Control*, 676–681.
16. Spencer, B.F., Jr., Dyke, S.J., Sain, M. K. and Carlson, J.D. (1997). "Phenomenological model of a magnetorheological damper." *Journal of Engineering Mechanics*, ASCE, **123**(3), 230–238.
17. Spencer, B.F. Jr., Nagarajaiah, S. (2003). "State of the art of structural control." *Journal of Structural Engineering*, ASCE, **129**(7), 845-856.
18. Symans, M.D., and Constantinou, M.C. (1999). "Semi-active control system for seismic protection of structures: a state-of-the art review." *Engineering Structures* **21**,469–487.
19. Yang, G., Spencer, B.F., Jr., Carlson, J.D. and Sain, M. K. (2002). "Large-scale MR fluid dampers: Modeling, and dynamic performance considerations." *Engineering Structures*, **20**, 309–323.
20. Yoshida, O. and Dyke, S.J. (2004). "Seismic control of a nonlinear benchmark building using smart dampers." *Journal of Engineering Mechanics*, ASCE, **130**(4), 386–392.
21. Yoshida, O. and Dyke, S.J. (2005), "Response Control of Full-Scale Irregular Buildings Using Magnetorheological Dampers", *Journal of Structural Engineering*, ASCE, **131**(5), 734-742.
22. Wen, Y.K. (1976). "Method of random vibration of hysteretic systems." *Journal of Engineering Mechanics*, **102**, 249–263.
23. Wereley, N.M., Pang, L., and Kamath, G. (1998). "Idealized hysteresis modeling of electrorheological and magnetorheological dampers." *Journal of Intelligent Material Systems and Structures*, **9**(8), 642–649.